

CompoDiff: Versatile Composed Image Retrieval With Latent Diffusion

Geonmo Gu^{*,1}, Sanghyuk Chun^{*,2}, Wonjae Kim², HeeJae Jun¹, Yoohoon Kang¹, Sangdoo Yun²

^{*} Equal contribution

¹NAVER Vision

²NAVER AI Lab

Abstract

This paper proposes a novel diffusion-based model, CompoDiff, for solving Composed Image Retrieval (CIR) with latent diffusion and presents a newly created dataset of 18 million reference images, conditions, and corresponding target image triplets to train the model. CompoDiff not only achieves a new zero-shot state-of-the-art on a CIR benchmark such as FashionIQ but also enables a more versatile CIR by accepting various conditions, such as negative text and image mask conditions, which are unavailable with existing CIR methods. In addition, the CompoDiff features are on the intact CLIP embedding space so that they can be directly used for all existing models exploiting the CLIP space. The code and dataset used for the training, and the pre-trained weights are available at <https://github.com/navervision/CompoDiff>.

1. Introduction

Imagine there is a virtual customer seeking a captivating cloth serendipitously found on social media but with different materials and colors. The customer needs a search engine that can process composed queries, e.g., the reference cloth image along with texts specifying the preferred material and color. This task has been recently formulated as *Composed Image Retrieval (CIR)* [36, 63] as shown in the top of Fig. 1. CIR systems offer the benefits of visually similar item searches as image-to-image retrieval [43], while providing a high degree of freedom to depict the desired item as text-to-image retrieval [18]. CIR also can be helpful for improving the search quality by iteratively taking user feedback by text conditions.

To train a model for CIR tasks, we need a dataset of triplets $\langle x_{i_R}, x_c, x_i \rangle^1$ consisting of a reference image (x_{i_R}), a condition (x_c), and the corresponding target image (x_i). However, obtaining such triplets can be costly and some-

¹Throughout this paper, we will use x to denote raw data and z to denote a vector encoded from x using an encoder, e.g., CLIP [44].



Figure 1. **Composed Image Retrieval (CIR) scenarios.** Top row shows an example of a standard CIR scenario. From the second to the bottom row, we present versatile CIR scenarios with mixed conditions (e.g., negative instruction and mask). All results are retrieved by our CompoDiff on LAION-5B images.

times impossible. Fortunately, existing CIR benchmarks [63, 36] provide such training triplets, which allows CIR models to achieve promising performance within the train-validation split of each dataset. However, the amount of the training triplet is not sufficient (e.g., 30K triplets for Fashion-IQ [63] and 36K triplets for CIRR [36]) for learning generalizable CIR models, as pointed out in [50]. Furthermore, the existing CIR methods usually consider a scenario where the condition (x_c) is given by a text (x_{c_T}). Therefore, the CIR models cannot handle more versatile conditions beyond a limited text one, e.g., complex text

conditions like negative prompts (x_{c_T}) or indicating where (x_{c_M}) the condition is applied (See Fig. 1). In short, the previous CIR models suffer from poor generalizability due to the small dataset scale and the limited types of conditions.

Recent methods [3, 4, 50] address the scalability issue of CIR datasets by leveraging external knowledge from models pre-trained on large-scale datasets such as CLIP [44]. CLIP4Cir [3, 4] fine-tunes the CLIP text encoder on the triplet dataset, but its zero-shot CIR performance is still lacking. In contrast, Pic2Word [50] only fine-tunes projectors on top of frozen CLIP encoders with image-text pairs instead of triplets, achieving zero-shot CIR ability. However, its performance on CIR benchmarks, such as FashionIQ, falls short due to the lack of triplet-based training.

To resolve the data scale issue, we synthesized a vast set of high-quality **18M** triplets of $\langle x_{i_R}, x_c, x_i \rangle$ by leveraging the large-scale pre-trained generative models such as OPT [65], and Stable Diffusion [48]. Our massive dataset, named **SynthTriplets18M**, is over 500 times larger than existing CIR datasets and covers a diverse and extensive range of conditioning cases. Our dataset leads to a significant performance improvement for any CIR model. *E.g.*, ARTEMIS [16] trained exclusively with our dataset achieves outperforming zero-shot performance with 40.62 average recalls in FashionIQ, against the fine-tuned counterpart of 38.17. We also achieve state-of-the-art FashionIQ and CIRR results by pre-training the previous best model on SynthTriplets18M and fine-tuning it on the target dataset.

We also introduce a diffusion-based CIR model to compose versatile and complex conditions, named Composed Image Retrieval with Latent Diffusion (CompoDiff). Motivated by recent advances in diffusion models [48, 47, 6], we train a latent diffusion model translating the embedding of the reference image (z_{i_R}) to the embedding of the target image (z_i) guided by the embedding of the given condition (z_c). Thanks to the classifier-free guidance of the diffusion model, CompoDiff can easily handle versatile and complex conditions. As Fig. 1, CompoDiff can search images from a given Eiffel Tower image by compositionally instructing “with cherry blossom” (text condition x_{c_T}), “without France” (negative text condition $x_{c_{T^-}}$) or specifying desired locations (mask condition x_{c_M}), which is not possible with standard CIR scenario with limited text condition x_{c_T} .

Another notable benefit of our method is the ability to control the conditions during inference, inherited from the nature of diffusion models: Users can adjust the weight of conditions to make the model focus on the user’s preference. Users can also manipulate the randomness of the models to vary the level of serendipity. Moreover, CompoDiff can control the inference speed with minimal sacrifice of retrieval performance, accomplished by adjusting the number of steps in the diffusion model. As a result, our model can be deployed in various scenarios with differ-

ent computation budgets. Note that all these controllability features can be achieved by controlling inference parameters of classifier-free guidance, without any model training.

Our contributions are as follows: (1) We generate SynthTriplets18M, a diverse and massive synthetic dataset of 18M triplets that can make CIR models achieve zero-shot generalizability. (2) We propose a diffusion-based CIR method (CompoDiff) that can handle versatile CIR scenarios with composed queries with high controllability. (3) CompoDiff shows significant zero-shot and comparable fine-tuned performances on FashionIQ and CIRR datasets. Also, we achieve a new state-of-the-art by pre-training the previous best model on our dataset. (4) Finally, we show the versatility of CompoDiff in the real-world zero-shot CIR scenario, *e.g.*, controllability or various conditions.

2. Related Works

Composed image retrieval. Until very recently, the mainstream CIR models were centered around multi-modal fusion methods, which combine image and text features extracted from separately trained visual and text encoders. For example, Vo *et al.* [62] and Yu *et al.* [64] used CNN and RNN, and Chen *et al.* [12] and Anwaar *et al.* [1] used CNN and Transformer for extracting their respective features. However, as shown in other vision-language tasks (*e.g.*, visual semantic embeddings [18, 58, 15, 8] for COCO Caption [9] retrieval), these separately trained encoders only on the target dataset are easily overwhelmed by large-scale pre-trained models, *e.g.*, CLIP [44], ALIGN [27] or BLIP [34].

Baldarati *et al.* [4] proposed CLIP4Cir, which consists of a first stage to fine-tune a CLIP text encoder and a second stage to train a late-fusion module called a Combiner, showed powerful performance. However, it still requires massive training triplets. Saito *et al.* [50] proposed a zero-shot CIR model, named Pic2Word, trained on aligned image-text pairs without using the triplet dataset at all. Pic2Word projects a CLIP image feature into the text embedding space and then uses the concatenated feature of the converted image feature and the given text condition as input of the text encoder. Pic2Word achieves reasonable CIR performances without direct training on the expensive triplet datasets. Since both methods freeze and use the CLIP visual encoder during the training process, the gallery (the set of images targeted for retrieval) features can be used exactly as it was extracted from the CLIP visual encoder. A detailed description of these models follows in Section 5.1.

All existing CIR models only focus on text conditions (x_{c_T}) (*e.g.*, the first row of Fig. 1). Compared to the previous CIR approaches, our method enables multiple various conditions (*e.g.*, the second to fourth rows of Fig. 1), but strong zero-shot and fine-tuned performances by employing (1) a massive synthetic triplet dataset and (2) a latent diffusion model with classifier-free guidance.

Dataset creation with diffusion models. A conventional data collection process for $\langle x_{i_R}, x_c, x_i \rangle$ is two-staged: collecting candidate reference-target image pairs and manually annotating the modification sentences by human annotators [5, 20, 19, 63, 36]. For example, FashionIQ [63] collects the candidate pairs from the same item category (*e.g.*, shirt, dress, and top) and manually annotates the relative captions by crowd workers. CIRR [36] gathers the candidate pairs from real-life images from the NLVR² dataset [59]. The data collection process for $\langle x_{i_R}, x_c, x_i \rangle$ inevitably becomes expensive and it makes scale CIR datasets difficult. We mitigate this issue by generating a massive synthetic dataset instead of relying on human annotators.

Recently, there have been attempts to generate synthetic data for improving model performances [6, 40, 56] by utilizing powerful generation ability by diffusion models [23, 48, 24]. Unlike previous attempts to synthesize training data points by GAN [13, 32, 51], recent diffusion model-based approaches show high-quality images and high controllability by text prompts (*e.g.*, by classifier-free guidance [24] and latent diffusion [48]). Particularly, Brooks *et al.* [6] proposed a generation process for $\langle x_{i_R}, x_c, x_i \rangle$ to train an image editing model. We scale up the dataset synthesis process of Brooks *et al.* from 450K triplets to 18M. We also make the triplets more diverse by employing the object-level modification process. We describe the details of the InstructPix2Pix dataset generation and our modification of the generation process in the upcoming Section 3.

3. SynthTriplets18M: Massive High-Quality Synthesized CIR Dataset

CIR needs a dataset with triplets $\langle x_{i_R}, x_c, x_i \rangle$ of a reference image (x_{i_R}), a condition (x_c), and the corresponding target image (x_i). Instead of collecting a dataset by humans, we propose to generate massive triplet data points by using large generative models. We follow the main idea of Instruct Pix2Pix [6]. First, we generate $\langle x_{t_R}, x_c, x_t \rangle$ where x_{t_R} is a reference caption, x_{ct} is a modification instruction text, and x_t is the modified caption by x_{ct} . We employ two strategies to generate $\langle x_{t_R}, x_c, x_t \rangle$: (1) We collect massive captions from the existing caption datasets and generate the modified captions by replacing the keywords in the reference caption. (2) We fine-tune a large language model, OPT-6.7B [65], on the generated caption triplets by Brooks *et al.* After generating massive triplets of $\langle x_{t_R}, x_c, x_t \rangle$, we generate images from the caption triplet using StableDiffusion [48] and Prompt-to-Prompt [22] following Brooks *et al.* [6]. We illustrate the overall generation process in Fig. 2.

Compared to manual dataset collections [63, 36], our approach can easily generate more diverse triplets even if a triplet rarely happens in reality (See the “pak choi tart” example in Fig. 2). Compared to the synthetic dataset by Brooks *et al.* [6], our dataset contains a larger number of

	IP2P [6]	SynthTriplets18M
$\langle x_{t_R}, x_c, x_t \rangle$	450k	60M
Unique object terms	47,345	586,369
$\langle x_{i_R}, x_c, x_i \rangle$ (Keyword-based)	-	11.4M
$\langle x_{i_R}, x_c, x_i \rangle$ (LLM-based)	1M	7.4M
$\langle x_{i_R}, x_c, x_i \rangle$ (Total)	1M	18.8M

Table 1. **Statistics of generated datasets.** We compare our SynthTriplets18M and the dataset by Instruct Pix2Pix (IP2P) in terms of the dataset statistics. $\langle x_{t_R}, x_c, x_t \rangle$ denotes the triplet of captions {original caption, modification instruction, and modified caption} and $\langle x_{i_R}, x_c, x_i \rangle$ denotes the triplet of {original image, modification instruction, and modified image}.

triplets (450k vs. 18M). Furthermore, as our caption triplets are synthesized based on keywords, our synthetic captions cover more diverse keywords than Instuct Pix2Pix (47k vs. 586k as shown in Table 1).

3.1. Keyword-based diverse caption generation

As the first approach to generating caption triplets, we collect captions from the existing caption datasets and modify the captions by replacing the object terms in the captions, *e.g.*, (“a strawberry tart is ...”, “covert strawberry to pak choi”, “a pak choi tart is ...”) in Fig. 2. For the caption dataset, We use the captions from COYO 700M [7], StableDiffusion Prompts² (user-generated prompts that make the quality of StableDiffusion better), LAION-2B-en-aesthetic (a subset of LAION-5B [52]) and LAION-COCO datasets [53] (synthetic captions for LAION-5B subsets with COCO style captions [9]. LAION-COCO less uses proper nouns than the real web texts).

We extract the object terms from the captions using a part-of-speech (POS) tagger, provided by Spacy³. After frequency filtering, we have 586k unique object terms. For each caption, we replace the object term with other similar keywords by using the CLIP similarity score. More specifically, we extract the textual feature of keywords using the CLIP ViT-L/14 text encoder, and we choose an alternative keyword from keywords that have a CLIP similarity between 0.5 and 0.7. By converting the original object to a similar object, we have caption pairs of $\langle x_{t_R}, x_t \rangle$.

Using the caption pair $\langle x_{t_R}, x_t \rangle$, we generate the modification instruction text x_{ct} based on a randomly chosen template from 47 pre-defined templates. We show examples of templates in Table 2 and the Appendix. After this process, we have the triplet of $\langle x_{t_R}, x_c, x_t \rangle$. We generate $\approx 30M$ triplets by the keyword-based method.

²<https://huggingface.co/datasets/Gustavosta/Stable-Diffusion-Prompts>

³<https://spacy.io>

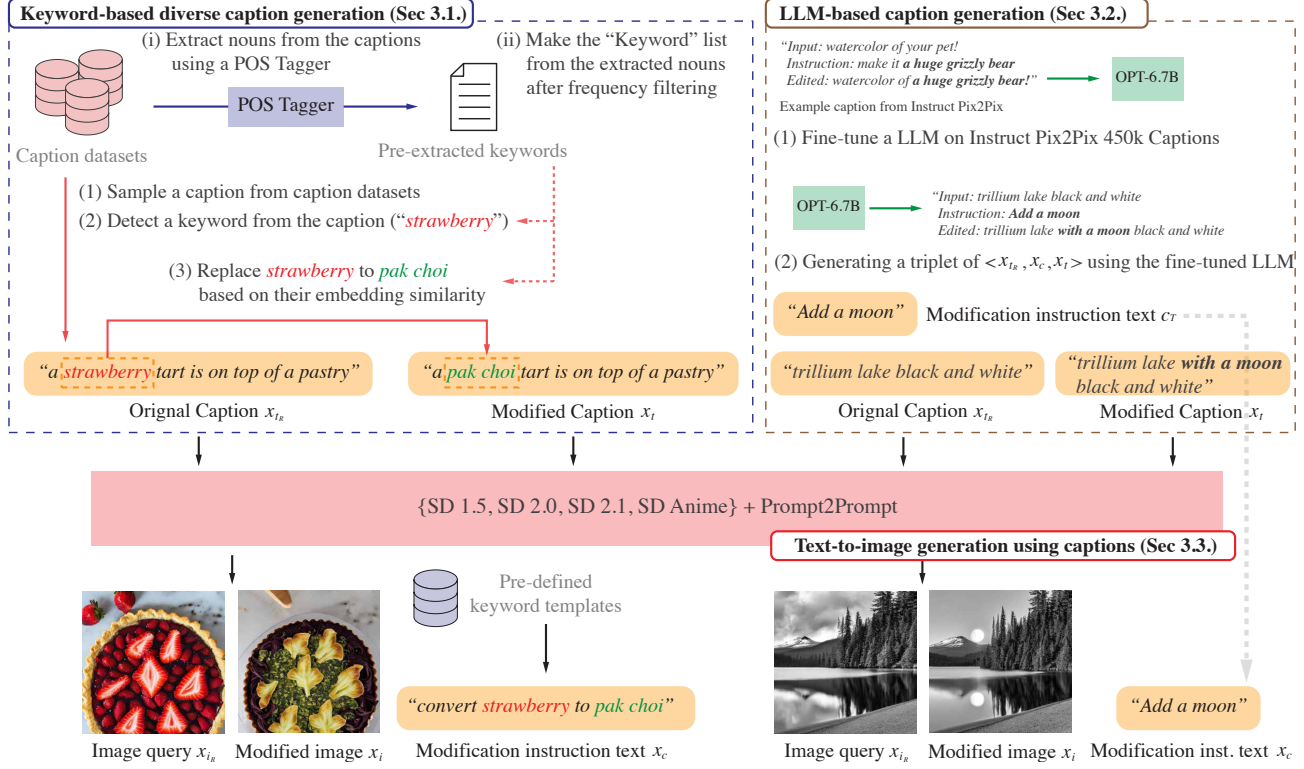


Figure 2. Overview of the generation process for SynthTriplets18M. $\langle x_{t_R}, x_c, x_i \rangle$ from $\langle x_{t_R}, x_c, x_t \rangle$. SD denotes StableDiffusion.

Templates to change \${source} to \${target}
“change \${source} to \${target}”
“alter \${source} to \${target}”
“\${target} is added after \${source} is removed”
“if it is \${target}”
...

Table 2. Example keyword converting templates. The full 47 templates are shown in Appendix A.2.

3.2. Amplifying Instruct Pix2Pix triplets by LLM

We also re-use the generated $\langle x_{t_R}, x_c, x_t \rangle$ by Instruct Pix2Pix. We amplify the number of Instruct Pix2Pix triplets by fine-tuning a large language model, OPT-6.7B [65], on the generated 452k caption triplets provided by Brook *et al.* Using the fine-tuned OPT, we generate ≈ 30 M triplets.

3.3. Triplet generation from caption triplets

We generate 60M caption triplets $\langle x_{t_R}, x_c, x_i \rangle$ by the keyword-based generation process and the LLM-based generation process (See Appendix A.1 for the statistics of the captions). Using the triplets, we generate 60M $\langle x_{t_R}, x_c, x_i \rangle$ by using state-of-the-art text-to-image generation models. Note that two captions do not have a guarantee to be semantically similar. Following Instruct Pix2Pix [6], we em-

ploy Prompt-to-Prompt [22], which aims to generate similar images for multiple generations by sharing cross-attention weights during the denoising steps of diffusion models.

We employ multiple state-of-the-art text-to-image generation models, including StableDiffusion (SD) 1.5, SD 2.0, SD 2.1, and SD anime models to generate diverse images not biased towards a specific model. We apply the CLIP-based filtering following Brook *et al.* [6] to remove the low quality $\langle x_{t_R}, x_c, x_i \rangle$ (See Appendix A.3 for details). After the filtering, we have 11.4M $\langle x_{t_R}, x_c, x_i \rangle$ from the keyword-based generated captions and 7.4M $\langle x_{t_R}, x_c, x_i \rangle$ from the LLM-based generated captions. It implies that the fidelity of our keyword-based method is higher than OPT fine-tuning in terms of text-to-image generation. As a result, our dataset contains 18.8M synthetic $\langle x_{t_R}, x_c, x_i \rangle$. We illustrate examples of SynthTriplets18M in Appendix A.4.

4. Method

In this section, we introduce our Composed Image Retrieval with Latent Diffusion (CompoDiff) to solve CIR tasks. Thanks to the massive and diverse synthetic dataset (Section 3), we can train a versatile model to handle various conditions based on a latent diffusion model [48], *i.e.*, the diffusion process is performed in the latent space, not the pixel space. We will describe the training and inference details and how CompoDiff handles various conditions.

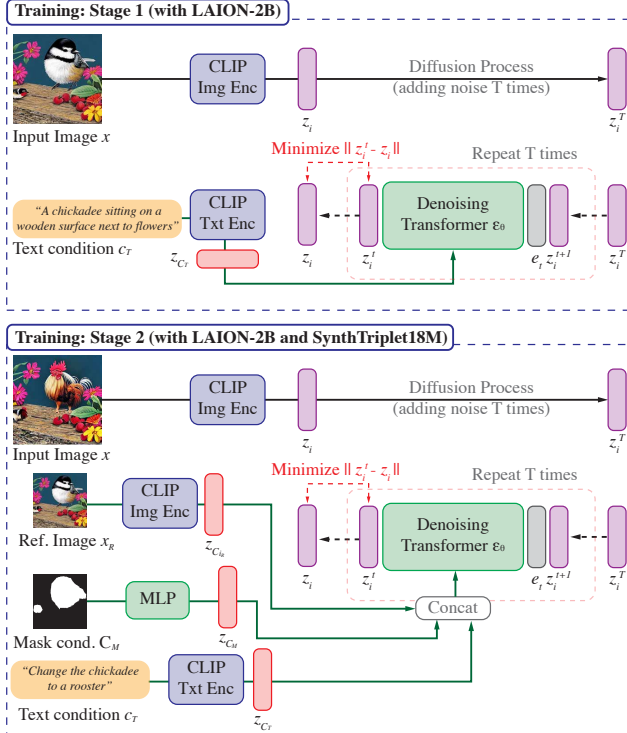


Figure 3. Overview of our two-stage training strategy. e_t denotes the embedding vector for timestamp t . For stage 2, we illustrate an example of all three conditions given. In practice, we randomly drop each condition to make CompoDiff handle various scenarios (e.g., text only, image-text composed query).

4.1. Training

We employ a two-staged pre-training fine-tuning strategy. In stage 1, we pre-train a transformer decoder to convert CLIP textual embeddings to CLIP visual embeddings with LAION 2B dataset [52] consisting of (image, text) pairs. This stage is similar to training the prior model in Dalle-2 [47], but our model takes only two tokens; a noised CLIP image embedding and an embedding for the diffusion timestep. In the prior model [47], 77 encoded text embeddings using the CLIP are employed as the input of the model, which increased the computational cost. However, our CompoDiff uses the 77 encoded text embeddings as conditions through cross-attention mechanisms, which speeds up the process by three times while maintaining similar performance (See Appendix D.5). Instead of using the noise prediction [23], we observe it is more stable to train the transformer decoder to predict the denoised x_i directly.

With CLIP image embeddings of an input image z_i , encoded CLIP text embeddings for text condition z_{c_T} , and the transformer ϵ_θ . The objective of the first stage is as follows:

$$\mathcal{L}_{\text{stage1}} = \mathbb{E}_{t \sim [1, T]} \|z_i - \epsilon_\theta(z_i^{(t)}, t | z_{c_T})\|^2 \quad (1)$$

In stage 2, we fine-tune the model for composed image

retrieval on SynthTriplets18M. By stage 2, we make the model able to generate modified image embeddings based on the context of a reference image, incorporating an instruction text and a mask. We use the CLIP visual and textual encoders to encode a reference image and a text condition (we also tested other text encoders in Appendix D.1). We generate masks by using a zero-shot text-conditioned segmentation model, ClipSeg [39]. We extract object terms from the given caption using a POS tagger, and we generate a segmentation map for each object term using ClipSeg. The mask is resized to 64×64 and projected to the same dimensional embedding as that of CLIP embeddings using an MLP. All conditions, including reference image embeddings, mask embeddings, and text embeddings are concatenated for the condition of the denoising Transformer.

We empirically observed that the knowledge from the LAION-2B dataset by stage 1 is easily forgotten during stage 2. To overcome the catastrophic forgetting, we introduce multi-task learning, with text-to-image learning and inpainting each accounting for 30%, and the remaining 40% of training done on the triplet dataset (SynthTriplets18M). The datasets used for text-to-image and inpainting are based on the 2B-scale LAION dataset to maintain the textual representational capability of our model learned in stage 1.

Let us define CLIP image embeddings of a reference image as z_{i_R} , CLIP image embeddings of a modified target image embeddings as z_{i_T} , and mask embeddings as z_{c_M} . We minimize the following objective:

$$\mathcal{L}_{\text{stage2}} = \mathbb{E}_{t \sim [1, T]} \|z_{i_T} - \epsilon_\theta(z_{i_T}^{(t)}, t | z_{c_T}, z_{i_R}, z_{c_M})\|^2. \quad (2)$$

We illustrate the overview of our training scheme in Fig. 3.

4.2. Inference

We apply Classifier-free guidance (CFG) [24], a commonly used technique in text-conditioned image generation methods for better text conditioning, for CompoDiff. We randomly drop each condition in stage 1 and stage 2 with 10% probability, except mask conditions. During inference, noisy image embeddings are denoised as follows:

$$\begin{aligned} \tilde{\epsilon}_\theta(z_i^{(t)}, t | z_{c_T}, z_{i_R}, z_{c_M}) &= \epsilon_\theta(z_i^{(t)}, t | \emptyset, \emptyset, z_{c_M}) \\ &+ w_I(\epsilon_\theta(z_i^{(t)}, t | \emptyset, z_{i_R}, z_{c_M}) - \epsilon_\theta(z_i^{(t)}, t | \emptyset, \emptyset, z_{c_M})) \\ &+ w_T(\epsilon_\theta(z_i^{(t)}, t | z_{c_T}, z_{i_R}, z_{c_M}) - \epsilon_\theta(z_i^{(t)}, t | \emptyset, z_{i_R}, z_{c_M})) \end{aligned} \quad (3)$$

We show the top-1 retrieved item by varying the image and text weights w_I and w_T from our LAION database in Fig. 4. By increasing w_I , our model behaves more like an image-to-image retrieval model. By increasing w_T , on the other hand, our model focuses more on the text condition ‘‘pencil sketch’’. We use $(w_I, w_T) = (1.5, 7.5)$ for our experiments. The retrieval performances by varying w_I and w_T are shown in Appendix D.5. We also describe how Eq. (3) is changed for negative texts in Appendix B.1.

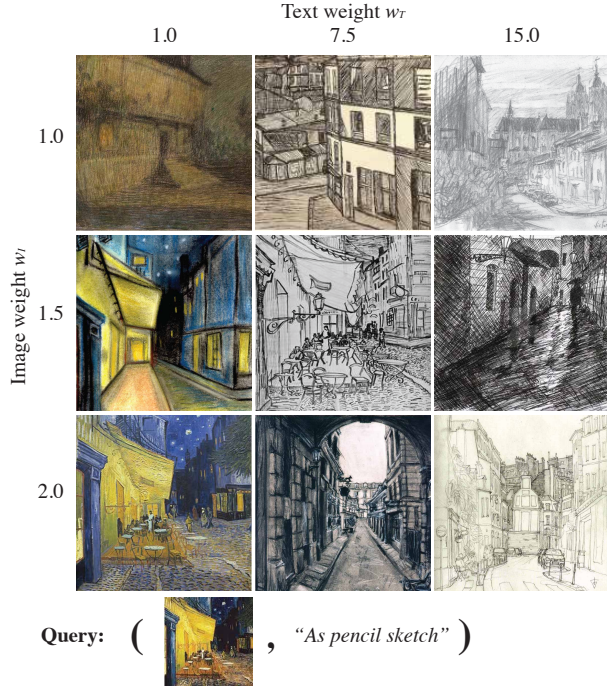


Figure 4. Controlling image and text weights for inference. We show example retrieval results on the LAION images by varying image and text weights, w_I and w_T in Eq. (3), respectively

5. Experiments

This section describes the experimental results on the zero-shot and fine-tuned composed image retrieval tasks for CompoDiff. We compare CompoDiff with the existing works on the standard CIR benchmarks (*e.g.*, FashionIQ [63] and CIRR [36]) and zero-shot benchmarks (*e.g.*, domain conversion and object compositional tasks, following [50]). We also provide qualitative examples of CompoDiff beyond performances, *e.g.*, handling versatile CIR scenarios. Our ablation study shows that by controlling inference hyperparameters, CompoDiff shows trade-offs in various scenarios (*e.g.*, performance vs. inference speed or focusing text more vs. image more). We also conducted experiments on the strengths of CompoDiff compared to other feature transformation models using diffusion models such as UniCLIP [47]. Unless otherwise noted, the model we used was trained with the training process described in Section 4 (See Appendix C.1 for the detailed hyperparameter settings). We additionally show the advanced version of CompoDiff by replacing the text encoder for text conditions (see a stage 2 training example in Fig. 3 for details) from the CLIP textual encoder to the combination of the CLIP textual encoder and T5-XL [45]. Details can be found in Appendix D.1.

5.1. Comparison with the State-of-the-Art

Comparison methods. We compare CompoDiff with three state-of-the-art CIR methods as follows:

- **CLIP4Cir** [4], also known as Combiner, involves a two-stage training process. First, the CLIP text encoder is fine-tuned by contrastive learning of z_c and $z_{i_R} + z_c$ in the CLIP embedding space. The second stage replaces $z_{i_R} + z_c$ to the learnable Combiner module. Only the Combiner module is trained during the second stage. Hence, its image embedding space is the same as the original CLIP space as CompoDiff.
- **ARTEMIS** [16] optimizes two similarities simultaneously. The implicit similarity is computed between the combined feature of z_i and z_c , and the combined one of z_{i_R} and z_c . The explicit matching is computed between z_i and z_c . ARTEMIS suffers from the same drawback as previous CIR methods, *e.g.* TIRG [62]: As it should compute combined feature of z_i and z_c , it is not feasible to use an approximate nearest neighbor search algorithm, such as FAISS [28]. This is not a big problem in a small dataset like FashionIQ, but it makes ARTEMIS infeasible in real-world CIR scenarios, *e.g.*, the entire LAION-5B dataset is the target database.
- **Pic2Word** [50] projects a visual feature into text embedding space, instead of combining them. Pic2Word performs a text-to-image retrieval by using the concatenated feature as the input of the CLIP textual encoder. As the projection module is solely trained on cheap paired datasets without expensive triplet datasets, it is able to solve CIR in a zero-shot manner.

For the qualitative comparison, we re-train Pic2Word on LAION-2B-en [52] because their pre-trained weight is not publicly available. We also demonstrate the effectiveness of our synthetic dataset by training the comparison methods on SynthTriplets18M with the default hyperparameters.

FashionIQ. FashionIQ, the most popular CIR benchmark, has (46.6k / 15.5k / 15.5k) (training / validation / test) images with three fashion categories: Shirt, Dress, and Top. Each category has 18k training triplets and 12k evaluation triplets of $\langle x_{i_R}, x_c, x_i \rangle$. Table 3 shows the comparison of CompoDiff with baselines. Following the standard choice, we use recall@K as the evaluation metric. “Zero-shot” means that the models are not trained on FashionIQ. ARTEMIS and CLIP4Cir are originally designed for the supervised setting, but, we trained them on our synthetic dataset for a fair comparison with our method. Namely, we solely train them on our dataset for the zero-shot benchmark and fine-tune the zero-shot weights on the FashionIQ training set for the supervised benchmark. As the result show, CompoDiff achieves a new state-of-the-art zero-shot performance and performs competitively in a supervised manner.

CIRR. As FashionIQ is fashion domain-specific, we also compare the methods on more generic images in CIRR. CIRR has 36k open-domain triplets divided into the train,

Method	Shirt		Dress		Toptee		Average		
	R@10	R@50	R@10	R@50	R@10	R@50	R@10	R@50	Avg.
Zero-shot									
Pic2Word [50]	20.00	40.20	26.20	43.60	27.90	47.40	24.70	43.70	34.20
ARTEMIS [16] trained w/ our dataset	30.70	50.43	33.52	46.54	35.49	47.01	33.24	47.99	40.62
CLIP4Cir [4] trained w/ our dataset	32.32	51.65	34.92	48.38	35.65	48.10	34.30	49.38	41.84
CompoDiff (ours)	37.69	49.08	32.24	46.27	38.12	50.57	36.02	48.64	42.33
CompoDiff (ours) w/ T5-XL [45]	38.10	52.48	<u>33.91</u>	<u>47.85</u>	40.07	52.22	37.36	50.85	44.11
Supervised									
JVSM [10]	12.00	27.10	10.70	25.90	13.00	26.90	11.90	26.60	19.25
CIRPLANT w/ OSCAR [37]	17.53	38.81	17.45	40.41	21.64	45.38	18.87	41.53	30.20
TRACE w/ BERT [26]	20.80	40.80	22.70	44.91	24.22	49.80	22.57	46.19	34.38
VAL w/ GloVe [11]	22.38	44.15	22.53	44.00	27.53	51.68	24.15	46.61	35.38
MAAF [17]	21.30	44.20	23.80	48.60	27.90	53.60	24.30	48.80	36.55
ARTEMIS [16]	21.78	43.64	27.16	52.40	29.20	54.83	26.05	50.29	38.17
CurlingNet [64]	21.45	44.56	26.15	53.24	30.12	55.23	25.90	51.01	38.46
CoSMo [33]	24.90	49.18	25.64	50.30	29.21	57.46	26.58	52.31	39.45
RTIC-GCN w/ GloVe [55]	23.79	47.25	29.15	54.04	31.61	57.98	28.18	53.09	40.64
DCNet [29]	23.95	47.30	28.95	56.07	30.44	58.29	27.78	53.89	40.84
AACL [60]	24.82	48.85	29.89	55.85	30.88	56.85	28.53	53.85	41.19
SAC w/ BERT [25]	28.02	51.86	26.52	51.01	32.70	61.23	29.08	54.70	41.89
MUR [12]	30.60	57.46	31.54	58.29	37.37	68.41	33.17	61.39	47.28
CLIP4Cir [4]	39.99	<u>60.45</u>	33.81	<u>59.40</u>	41.41	<u>65.37</u>	38.32	<u>61.74</u>	<u>50.03</u>
ARTEMIS [16] trained w/ our dataset	32.17	53.32	34.80	48.10	36.58	47.63	34.52	49.68	42.10
CLIP4Cir [4] trained w/ our dataset	37.21	60.71	42.75	60.50	<u>42.98</u>	65.49	40.98	62.23	51.61
CompoDiff (ours)	40.88	53.06	35.53	49.56	41.15	54.12	39.05	52.34	46.31
CompoDiff (ours) w/ T5-XL [45]	<u>40.65</u>	<u>57.14</u>	36.87	57.39	43.93	61.17	<u>40.48</u>	58.57	49.53

Table 3. **Comparisons on FashionIQ validation set.** We report two scenarios. The “Zero-shot” scenario performs a composed-image retrieval using a model not trained on the FashionIQ dataset, while models are trained on FashionIQ for the “Supervised” scenario. “train w/ our dataset” denotes that a model is trained on our synthetic dataset (Section 3).

validation, and test sets in 8:1:1 split. Table 4 shows the results, and all experimental settings were identical to FashionIQ. Similar to FashionIQ, CompoDiff also achieves a new state-of-the-art CIRR zero-shot performance. It is noteworthy that CLIP4Cir performs great in the supervised setting but performs worse than CompoDiff in the zero-shot setting. We presume that the fine-tuned CLIP4Cir text encoder is overfitted to long-tailed CIRR captions. It is partially supported by our additional experiments using the combination of CLIP encoder and T5-XL text encoder [45]; a better understanding of complex texts provides better performances (Details and more results are in Appendix D.1).

For both datasets, we achieve state-of-the-art by fine-tuning the CLIP4Cir model trained on our dataset to the target dataset. It shows the benefits of our dataset compared to the limited number of CIR triplet datasets.

Additional tasks. We also conduct additional zero-shot evaluation results following Saito *et al.* [50]. We report the results of a domain conversation task on ImageNet-R [21] (Appendix D.2), and an object compositional task on

MS-COCO [35] (Appendix D.3). In summary, CompoDiff outperforms Pic2Word on ImageNet-R, but not on COCO. Detailed discussions are in Appendix D.

5.2. Qualitative examples

We qualitatively show the versatility of CompoDiff for handling various conditions. For example, CompoDiff not only can handle a text condition, but it can also handle a *negative* text condition (*e.g.*, removing specific objects or patterns in the retrieval results), masked text condition (*e.g.*, specifying the area for applying the text condition). CompoDiff even can handle all conditions simultaneously (*e.g.*, handling positive and negative text conditions with a partly masked reference image at the same time). To show the quality of the retrieval results, we conduct a zero-shot CIR on entire LAION dataset [52] using FAISS [28] for simulating billion-scale CIR scenarios. We show an example in Fig. 1 and more examples are shown in Appendix D.4.

Fig. 5 shows qualitative examples of zero-shot CIR results by Pic2Word and CompoDiff. CompoDiff results in semantically high-quality retrieval results (*e.g.*, understand-

Method	R@1	R@5	R@10	R@50	R _s @1	R _s @2	R _s @3	Avg(R@1, R _s @1)
Zero-shot								
Pic2Word [50]	23.90	51.70	65.30	87.80	-	-	-	-
ARTEMIS [16] trained w/ our dataset	12.75	33.84	47.75	80.20	21.95	43.88	62.06	17.35
CLIP4Cir [4] trained w/ our dataset	12.82	36.83	48.19	81.91	24.12	46.47	63.07	18.47
CompoDiff (ours)	18.24	53.14	70.82	90.35	27.51	48.30	65.54	22.88
CompoDiff (ours) w/ T5-XL [45]	<u>19.37</u>	53.81	72.02	90.85	28.96	49.21	67.03	24.17
Supervised								
TIRG [62]	14.61	48.37	64.08	90.03	22.67	44.97	65.14	18.64
TIRG + LastConv [62]	11.04	35.68	51.27	83.29	23.82	45.65	64.55	17.43
MAAF [17]	10.31	33.03	48.30	80.06	21.05	41.81	61.60	15.68
MAAF + BERT [17]	10.12	33.10	48.01	80.57	22.04	42.41	62.14	16.08
MAAF-IT [17]	9.90	32.86	48.83	80.27	21.17	42.04	60.91	15.54
MAAF-RP [17]	10.22	33.32	48.68	81.84	21.41	42.17	61.60	15.82
CIRPLANT [37]	15.18	43.36	60.48	87.64	33.81	56.99	75.40	24.50
CIRPLANT w/ OSCAR [37]	19.55	52.55	68.39	92.38	39.20	63.03	79.49	29.38
ARTEMIS [16]	16.96	46.10	61.31	87.73	39.99	62.20	75.67	28.48
CLIP4Cir [4]	<u>38.53</u>	69.98	81.86	95.93	68.19	85.64	94.17	53.36
ARTEMIS [16] trained w/ our dataset	18.85	51.44	68.01	91.93	38.85	62.00	77.68	28.85
CLIP4Cir [4] trained w/ our dataset	39.99	73.63	86.77	96.55	68.41	86.12	94.80	54.20
CompoDiff (ours)	21.30	55.01	72.62	91.49	33.74	55.25	74.81	27.52
CompoDiff (ours) w/ T5-XL [45]	22.35	54.36	73.41	91.77	35.84	56.11	76.60	29.10

Table 4. Comparisons on CIRR Test set. Details are the same as Table 3.

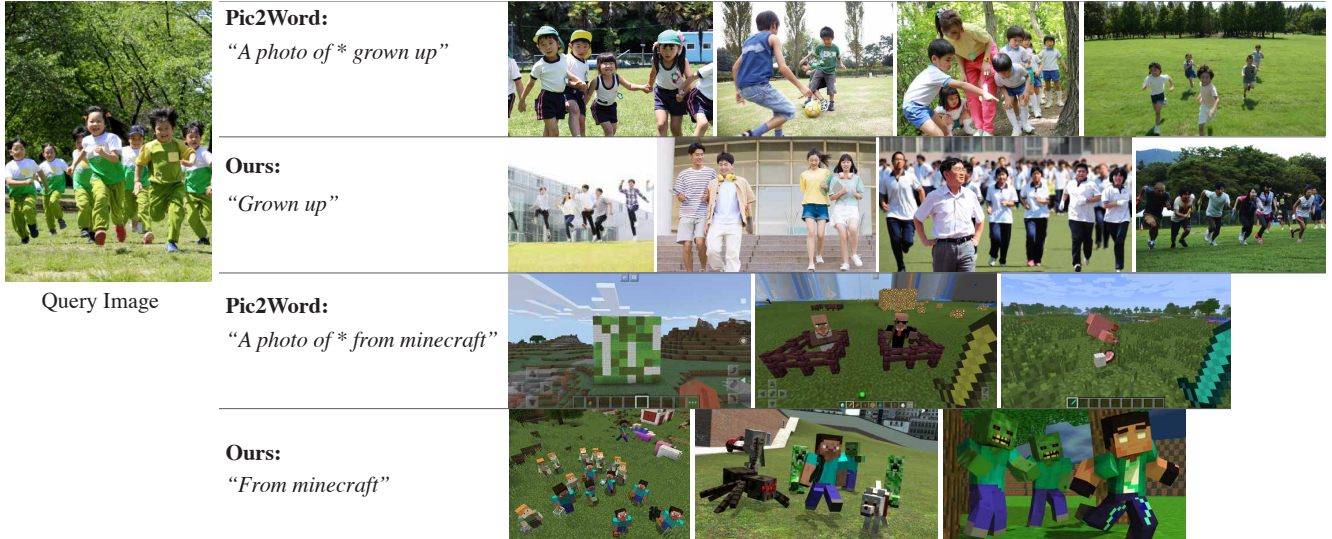


Figure 5. Qualitative comparison of zero-shot CIR for Pic2Word and CompoDiff. We conduct CIR on LAION with two composed query scenarios. As Pic2Word cannot take a simple instruction, we made a simple modification for the given instruction as shown. Pic2Word inserts the image-converted text embedding at the position of * in the original text embedding.

ing the “crowdedness” of the query image and the meaning of the query text at the same time). However, Pic2Word shows poor understanding of the given queries, resulting in unfortunate retrieval results (*e.g.*, ignoring “grown up” of text query, or the “crowdedness” of the query image). We provide the details and more examples in Appendix D.4.

Finally, it is worth noting that CompoDiff generates a feature belonging to the CLIP space. It means that we can apply the unCLIP generator [47] on our composed features. We compare the retrieval results from the LAION dataset and the generated images in Appendix D.6. CompoDiff can manipulate the given input reflecting the given conditions.

5.3. Ablation Studies

We provide ablation studies for our design choices, including the architecture design, the trade-off between the denoising step (*i.e.*, inference time) and performances, and the retrieval performances by varying the image and text weights (w_I and w_T). In summary, our design choice shows $\times 3$ faster inference time than the prior model [47] but better text-to-image retrieval performances on COCO. Also, we observe that CompoDiff performs better by increasing the de-noising step, but empirically shows good performances with the de-noising step size 5. Due to the page limit, the full results can be found in Appendix D.5.

6. Conclusion

In this paper, we have introduced Composed Image Retrieval with Latent Diffusion (CompoDiff), a novel method for solving complex composed image retrieval (CIR) tasks. We have created a large and diverse dataset named SynthTriplets18M, consisting of 18M triplets of images, modification texts, and modified images. Our model has demonstrated impressive zero-shot CIR capabilities, as well as remarkable versatility in handling diverse conditions, such as negative text or image masks. Additionally, by pre-training previous state-of-the-art CLIP4Cir on SynthTriplets18M and fine-tuning it on each target dataset, we have achieved state-of-the-art performance in both FashionIQ and CIRR benchmarks. We strongly encourage future researchers to leverage our dataset for advancing the field of CIR.

Societal Impact

Our work is primarily focused on solving complex composed image retrieval (CIR) challenges and is not designed for image editing purposes. However, we are aware that with the use of additional public resources, such as the community version of the unCLIP feature decoder [47], our method can potentially be utilized as an image editing method. We would like to emphasize that this unintended application is not the primary objective of our research, and we cannot guarantee the effectiveness or safety of our method in this context.

It is important to note that we have taken steps to mitigate potential risks associated with the unintended use of our method for image editing. For instance, we applied NSFW filters to filter out potentially malicious samples during the creation of SynthTriplets18M. Nevertheless, we recognize the need for continued research into the ethical and societal implications of AI technologies and pledge to remain vigilant about potential unintended consequences of our work.

Appendix

In this additional document, we describe the details of our data generation process in Appendix A, including the statistics of our generated dataset (Appendix A.1), the full keyword converting templates (Appendix A.2), the dataset filtering process (Appendix A.3) and examples of SynthTriplets18M (Appendix A.4). We also provide more details for CompoDiff in Appendix B, including how to handle negative texts (Appendix B.1) and denoising Transformer details (Appendix B.2). Appendix C contains more experimental details of CompoDiff, such as the implementation details (Appendix C.1) and the details of LAION dataset for retrieval (Appendix C.2). Finally, we provide more experimental results in Appendix D, including the impact of the text encoder (Appendix D.1), the domain conversion task (Appendix D.2), the object compositional task (Appendix D.3), more qualitative examples (Appendix D.4), ablation study (Appendix D.5) and generation examples by using the unCLIP generator (Appendix D.6).

A. More Details for SynthTriplets18M

A.1. Dataset Statistics

We show the statistics of our generated caption dataset (*i.e.*, before text-to-image generation, x_{t_R} and x_t). We use the CLIP tokenizer to measure the statistics of the captions. Fig. A.1 shows the cumulative ratio of captions with tokens less than X. About half of the captions have less than 13 tokens, and 90% of the captions have less than 20 tokens. Only 0.8% of the captions have more than 40 tokens.

We also compare our dataset, FashionIQ [63] and CIRR [36] in terms of the token statistics of instructions (*i.e.*, x_c). Fig. A.2 shows that our dataset has relatively shorter instructions than other human-annotated instructions. We presume that this is why CompoDiff performs better when fine-tuning on the target dataset.

A.2. The Full Keyword Converting Templates

Table A.1 shows the 47 templates to convert keywords.

A.3. Filtering process

In the first iteration of our generation process, we generated approximately 60 million triplet images. Then, we apply a CLIP-based filter to filter out low-quality triplets. We filter the generated images for an image-image CLIP threshold of 0.70 to ensure that the images are not too different, an image-caption CLIP threshold of 0.2 to ensure that the images correspond to their captions, and a directional CLIP similarity of 0.2 to ensure that the change in before/after captions correspond with the change in before/after images. Additionally, in the case of keyword-based data generation, we filter out for a keyword-image CLIP threshold of 0.20

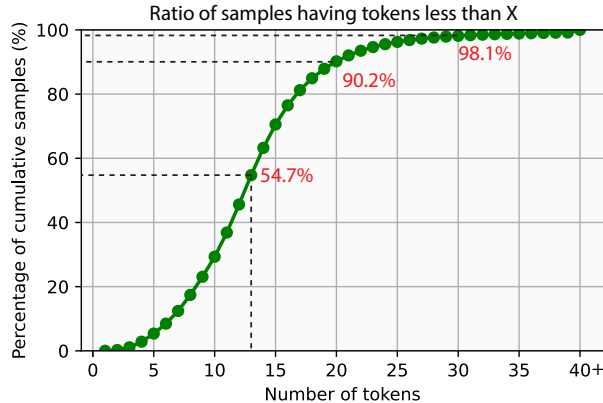


Figure A.1. **Statistics of our captions.** We show the population of our captions by the number of tokens per caption. We include captions having larger than 40 tokens in “40+”.

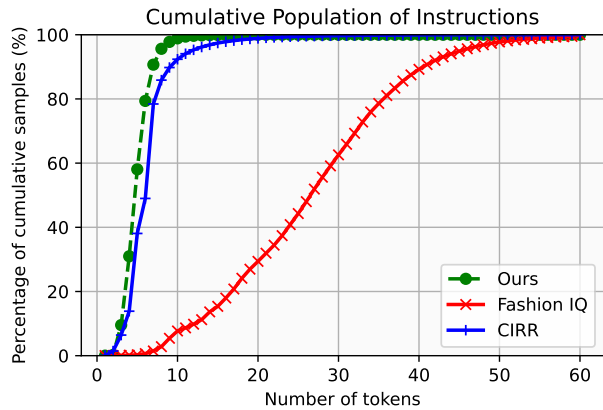


Figure A.2. **Statistics of instructions for three CIR datasets.** We show the population of instruction captions (e.g., “change A to B”) by the number of tokens. We include captions having larger than 60 tokens in “60”.

to ensure that images contain the context of the keyword, and in the case of instruction-based data generation, we filter out for an instruction-modified image CLIP threshold of 0.20 to ensure that an image is consistent with the given instructions.

A.4. More examples of SynthTriplets18M

We illustrate examples of SynthTriplets18M in Fig. A.3. Our dataset can express the change of overall context (e.g., “make the landscape a cityscape”), the seasonal change (e.g., “make it sprint”), the change of mood (e.g., “make it a watercolor”), and the change of local objects (e.g., “have the person be a dog”).

Templates to change \${source} to \${target}

```

“replace ${source} with ${target}”
“substitute ${target} for ${source}”
“change ${source} to ${target}”
“${target}”
“apply ${target}”
“add ${target}”
“exchange ${source} with ${target}”
“alter ${source} to ${target}”
“convert ${source} to ${target}”
“transform ${source} into ${target}”
“swap ${source} for ${target}”
“replace ${source} with ${target}”
“remodel ${source} into ${target}”
“redesign ${source} as ${target}”
“update ${source} to ${target}”
“revamp ${source} into ${target}”
“if it is ${target}”
“substitute ${target} for ${source}”
“modify ${source} to become ${target}”
“turn ${source} into ${target}”
“alter ${source} to match ${target}”
“customize ${source} to become ${target}”
“adapt ${source} to fit ${target}”
“upgrade ${source} to ${target}”
“change ${source} to match ${target}”
“tweak ${source} to become ${target}”
“amend ${source} to fit ${target}”
“${target} is the new option”
“choose ${target} instead”
“${target} is the updated version”
“use ${target} from now on”
“${target} is the new choice”
“opt for ${target}”
“${target} is the updated option”
“${target} is the new selection”
“${target} is the new option available”
“${target} is the updated choice”
“${source} is replaced with ${target}”
“${source} is removed and ${target} is added”
“${target} is introduced after ${source} is removed”
“${source} is removed and ${target} takes its place”
“${target} is added after ${source} is removed”
“${source} is removed and ${target} is introduced”
“${target} is added in place of ${source}”
“${target} is introduced after ${source} is retired”
“${target} is added as a replacement for ${source}”
“${target} is introduced as the new option after
 ${source} is removed”

```

Table A.1. **The full 47 keyword converting templates.**

B. More Details for CompoDiff

B.1. Details for negative text

CompoDiff employs a diffusion probabilistic model, allowing us to leverage the advantages of the diffusion model as described in Section 4.2 (Classifier-free guidance). Let us define the null embeddings for a text as \mathcal{O}_{ct} and for an image as \mathcal{O}_{i_R} . Then, we can rewrite Eq. (3) as follows:



"chinese landscape watercolor painting"



"chinese cityscape watercolor painting"



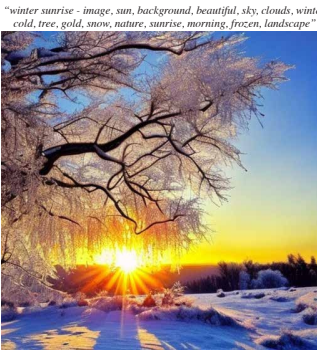
"ralph hedley ~ watering the garden ~ (english, 1851-1913)"



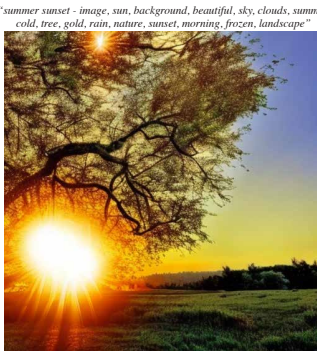
"ralph hedley ~ watering the swamp ~ (english, 1851-1913)"

"make the landscape a cityscape"

"make the garden a swamp"



"winter sunrise - image, sun, background, beautiful, sky, clouds, winter;" "summer sunset - image, sun, background, beautiful, sky, clouds, summer, cold, tree, gold, snow, nature, sunrise, morning, frozen, landscape"



"mark-keathley-painting-winter"

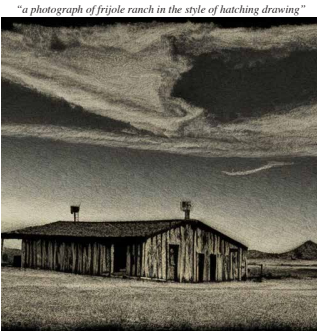


"mark-keathley-painting-spring"



"change the season to summer"

"make it spring"



"a photograph of frijoles ranch in the style of hatching drawing"



"a photograph of frijoles ranch in the style of 4k high resolution images"



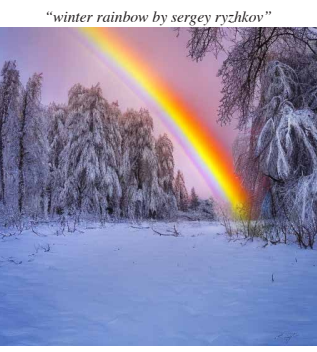
"amazing digital paintings by flore maquin - II"



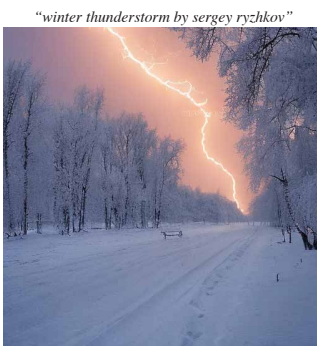
"amazing watercolors by flore maquin - II"

"4k high resolution images is the new choice"

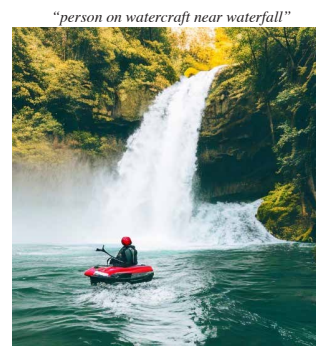
"make it a watercolor"



"winter rainbow by sergey ryzhkov"



"winter thunderstorm by sergey ryzhkov"



"person on watercraft near waterfall"



"dog on watercraft near waterfall"

"make it a thunderstorm"

"have the person be a dog"

Figure A.3. **Examples of SynthTriplets18M.** We show examples of $\langle x_{i_R}, x_c, x_i \rangle$, i.e., $\{ \text{original image}, \text{modification instruction}, \text{and modified image} \}$, as well as the generation prompt for x_{i_R} and x_i .

$$\begin{aligned}
\tilde{\epsilon}_\theta(z_i^{(t)}, t | z_{c_T}, z_{i_R}, z_{c_M}) &= \epsilon_\theta(z_i^{(t)}, t | \emptyset_{c_T}, \emptyset_{i_R}, z_{c_M}) \\
&+ w_I(\epsilon_\theta(z_i^{(t)}, t | \emptyset_{c_T}, z_{i_R}, z_{c_M}) - \epsilon_\theta(z_i^{(t)}, t | \emptyset_{c_T}, \emptyset_{i_R}, z_{c_M})) \\
&+ w_T(\epsilon_\theta(z_i^{(t)}, t | z_{c_T}, z_{i_R}, z_{c_M}) - \epsilon_\theta(z_i^{(t)}, t | \emptyset_{c_T}, z_{i_R}, z_{c_M}))
\end{aligned} \tag{B.1}$$

For \emptyset_{c_T} , CLIP textual embeddings for empty text ("") is used and we employ an all-zero vector for \emptyset_{i_R} . When a negative text is employed, we simply replace \emptyset_{i_R} with the CLIP textual embeddings c_T^- for the negative text.

B.2. Denoising Transformer implementation details

Instead of using the denoising U-Net [48], we employ a simple transformer architecture for the denoising procedure. We empirically observe that our transformer architecture works slightly better than the U-Net architecture, but is a lot simpler. Since the exhaustive architecture search is expensive, we did not test various alternatives, but we fix our denoising module as a Transformer. We use the multi-head self-attention blocks as the original Transformer [61], where the depth, the number of heads, and the dimensionality of each head are set to 12, 16, and 64, respectively.

We use two inputs as the input of the denoising Transformer: a noisy visual embedding and a time step embedding. The conditions (*e.g.*, text conditions, mask conditions, image conditions) are applied only to the cross-attention layer of the Transformer, so it is computationally efficient even if the number of conditions becomes larger. Our implementation is similar to the “DiT block with cross-attention” by Peebles *et al.* [42], but our implementation handles much various conditions, such as text conditions, mask conditions, and image conditions.

C. More Experimental Details

C.1. Implementation details

We report the detailed hyperparameters in Table C.1. All models were trained using AdamW [38] with $\beta_1 = 0.9$ and $\beta_2 = 0.999$. For computationally efficient training, we pre-computed CLIP visual embeddings of the entire image from our training dataset. Since our training dataset was sufficiently large, we did not use any image augmentation methods to extract CLIP visual embeddings. Since the text as a condition can vary each time in training according to the 47 templates (Table A.1), we do not precompute any textual embeddings. In the case of keyword-based generated triplets, we are able to randomly switch query and modified images during training because the instruction for keyword-based triplets is generated according to the 47 templates.

C.2. LAION dataset for retrieval

We employed all images from the LAION 5B [52] dataset to build a search index. We use the 2B English caption subset of LAION for training stages. We use the full

LAION-5B images for the qualitative evaluation of zero-shot CIR in the later section.

D. More Experimental Results

D.1. Impact of text encoder

As shown in Balaji *et al.* [2], using a text-oriented model such as T5 [46] in addition to the CLIP textual encoder results in improved performance of text-to-image generation models. Motivated by this observation, we also use both the CLIP textual encoder and the language-oriented encoder. We also observed the positive effect of the text-oriented model and experimental results showed that T5-XL, which has 3B parameters, could improve the performance by a large margin in the overall evaluation metrics. As described in Appendix C.1, all training text embeddings are extracted at every iteration. To improve computational efficiency, we reduced the number of input tokens of the T5 models to 77, as in CLIP (as shown in Fig. A.1 and Fig. A.2, most of the captions in our dataset have lengths less than 77).

We compare different text encoder choices on four different tasks (ImageNet-R and COCO for domain conversion tasks – see Appendix D.2 and Appendix D.3 for details – and Fashion IQ and CIRR datasets for CIR tasks) with zero-shot and fine-tuned scenarios. We report all experimental results in Table D.1. When using the CLIP textual encoder and the T5-XL were used together, the experimental results improved by a large margin. We suspect that this is because the strong T5 encoder can help the CLIP text encoder to better understand given captions. Interestingly, we observe that using T5 alone degrades the performance even compared to using the CLIP textual encoder alone. We suspect that this is because T5-XL is specified for long text sequences (*e.g.*, larger than 100 tokens) and text-only data. On the other hand, our caption dataset has an extremely short average length (see Fig. A.1 and Fig. A.2), which is not specialized by T5. Also, our dataset is based on captions, paired with an image; we also need to consider image information to understand the given caption, but we cannot handle image information alone with T5.

D.2. Domain conversion task

Following Pic2Word [50], we evaluate the ability to compose domain information. We use ImageNet [49] as reference images and ImageNet-R [21] as the target images. Domains of ImageNet-R (cartoon, origami, toy, and sculpture) are used as text conditions with simple prompt engineering, *e.g.*, we use “as a cartoon, drawing”, “as an origami”, “as a toy, plastic model”, and “as a sculpture” for text conditions. As described in Table D.2, CompoDiff shows the best results in the ImageNet-R benchmark. We also observe that by training models on our dataset, the zero-shot ARTEMIS [16] and CLIP4Cir [4] show competi-

	Stage1	Stage2	Fine-tuning
Diffusion steps	1000	1000	1000
Noise schedule	cosine	cosine	cosine
Sampling steps	10	10	10
Sampling variance method	DDIM [57]	DDIM [57]	DDIM [57]
Dropout	0.1	0.1	0.1
Weight decay	6.0e-2	6.0e-2	6.0e-2
Batch size	4096	2048	2048
Iterations	1M	200K	50K
Learning rate	1e-4	1e-5	1e-5
Optimizer	AdamW [38]	AdamW [38]	AdamW [38]
EMA decay	0.9999	0.9999	0.9999
Input tokens	$z_i^{(t)}, t$	$z_i^{(t)}, t$	$z_i^{(t)}, t$
Conditions	z_{c_T}	$z_{c_T}, z_{i_R}, z_{c_M}$	z_{c_T}, z_{i_R}
Training dataset	LAION 2B English [52]	LAION 2B English [52], Our dataset	FashionIQ [63] or CIRR [36] trainset
Image encoder	CLIP-L/14 [44]	CLIP-L/14 [44]	CLIP-L/14 [44]
Text encoder	CLIP-L/14 [44]	CLIP-L/14 [44]	CLIP-L/14 [44]
Denoiser depth	12	12	12
Denoiser heads	16	16	16
Denoiser head channels	64	64	64

Table C.1. **Hyperparameters.** A model trained by Stage 1 and Stage 2 is equivalent to “Zero-shot” in the main table. A “supervised model” is the same as the fine-tuned version.

	T5-XL	CLIP + T5-XL	CLIP
Zero-shot			
ImageNet-R R@10	11.14	13.31	13.18
COCO R@1	6.82	8.77	8.71
FashionIQ Avg Recall	38.20	44.11	42.33
CIRR Avg Recall	16.41	24.17	22.88
Supervised			
FashionIQ Avg Recall	41.48	49.53	46.31
CIRR Avg Recall	20.39	29.10	27.52

Table D.1. **Impact of text encoder.** We compare CompoDiff with different text encoders: (1) the T5-XL text encoder, (2) the combination of the CLIP and T5-XL text encoders, and (3) the CLIP text encoder. Four different datasets are evaluated for three models.

tive results with our method.

Note that we have reported three different results for Pic2Word. Pic2Word (reported) is the result of the original Pic2Word paper [50]. We reproduce Pic2Word by using the ConceptualCaption-3M dataset [54] and the LAION 2B-en dataset. Despite increasing the size of the dataset from 3M to 2B, we do not observe significant performance changes between CC-3M and LAION-trained Pic2Word.

D.3. Object compositional task

This section focuses on assessing the capability to generate an instance by providing an image and additional textual descriptions of other scenes or objects. Following

Pic2Word [50], we randomly select and crop an object from the image of the COCO validation set [35] and apply its instance mask to remove the background. The text specification is based on the list of object classes present in the image, which is then combined into a single sentence using commas. Since the experimental protocol requires a random selection of objects, we repeated the experiment five times and reported full results in Table D.3. Here, we use the average of CLIP visual embeddings and textual embeddings (**Image + Text**) as a baseline. Interestingly, we observe that the simple **Image + Text** approach shows the best performance out of all zero-shot approaches, including Pic2Word and CompoDiff. This could be due to two reasons. First, our dataset does not contain multiple changes or multiple objects in a single text guidance Section 3. This may limit the performance of CompoDiff limited. Second, the random object selection process could select very small objects with high probability (almost half of the objects are smaller than 1% of the full image [30]), which can make the edited images noisy. As shown in the table, we observe that the variances of the benchmark are not negligible; it can show the noisiness of the object compositional task by Pic2Word [50].

D.4. More qualitative examples

Open world zero-shot CIR comparisons with Pic2Word. We illustrate further comparisons with Pic2Word in Fig. D.1. Here, we can draw the same conclusions as in the main text: Pic2Word often cannot understand images

	Cartoon		Origami		Toy		Sculpture		Average	
	R@10	R@50	R@10	R@50	R@10	R@50	R@10	R@50	R@10	R@50
Pic2Word [50] (reported)	8.0	21.9	13.5	25.6	8.7	21.6	10.0	23.8	10.1	23.2
Pic2Word (CC-3M [54])	7.35	18.53	12.79	25.54	10.39	22.96	10.24	23.76	10.19	22.70
Pic2Word (LAION 2B-en [52])	8.17	20.86	14.08	25.06	8.73	22.07	10.43	23.63	10.35	22.91
ARTEMIS [16] w/ our dataset	11.42	23.81	15.49	25.44	11.21	24.01	10.84	21.07	12.24	23.58
CLIP4Cir [4] w/ our dataset	10.90	24.12	16.08	25.60	11.01	23.57	10.45	21.86	12.11	23.79
CompoDiff (T5-XL)	8.43	20.40	15.73	25.69	11.19	22.48	9.19	18.45	11.14	21.76
CompoDiff (CLIP, T5-XL)	12.91	24.40	17.22	26.40	11.57	26.11	11.53	22.54	13.31	24.86
CompoDiff (CLIP)	13.21	24.06	17.03	26.17	11.22	26.25	11.24	22.96	13.18	24.86

Table D.2. **Domain conversion task on ImageNet-R.** All numbers, except Pic2Word (reported), are reproduced numbers. The first three rows show the effect of different training datasets. We also report zero-shot results of ARTEMIS and CLIP4Cir trained by our dataset in the fourth and fifth rows.

	Trial 1	Trial 2	Trial 3	Trial 4	Trial 5	Average
Image + Text	11.04	11.40	11.35	11.35	11.19	11.27
Pic2Word (GCC3M)	11.00	11.29	10.72	10.72	11.00	10.95
Pic2Word (LAION 2B-en)	10.58	10.39	10.58	10.56	10.47	10.52
ARTEMIS w/ our dataset	8.51	9.1	8.65	8.75	8.32	8.67
CLIP4Cir w/ our dataset	9.02	9.27	8.91	9.02	8.83	9.01
CompoDiff (T5-XL)	6.71	7.01	6.89	6.92	6.58	6.82
CompoDiff (CLIP, T5-XL)	8.90	8.82	8.38	9.11	8.64	8.77
CompoDiff (CLIP)	8.69	8.95	8.42	8.90	8.57	8.71

Table D.3. **Object compositional task on MS-COCO.** We report 5 different runs of COCO object compositional task proposed by Pic2Word [50]. Details for each method are the same as Table D.2.

or instructions (*e.g.*, ignores the “crowdedness” of the images, or retrieves irrelevant images such as images with a woman in the last example). All retrieved results in our paper were obtained using Pic2Word trained on the LAION 2B-en dataset (*i.e.*, Pic2Word LAION 2B-en in Table D.2).

More versatile CIR examples on LAION. We illustrate more qualitative examples in Fig. D.3, Fig. D.4, Fig. D.5, and Fig. D.6. We will describe the details of “Generated by unCLIP” in the later section.

D.5. Ablation study

How to handle text input? CompoDiff does not take CLIP textual embeddings for text guidance as input tokens of the denoising Transformer but as a condition of cross-attention. Our design choice allows for faster throughput compared to the counterpart that takes CLIP textual embeddings directly as input tokens. We compare the impact of different design choices for handling textual embeddings. First, we evaluate the “Prior” model which converts CLIP textual embeddings into CLIP visual embeddings and proposed in unCLIP [47] (we use a public community model⁴ because the official model is not yet publicly available).

⁴<https://huggingface.co/kakaobrain/karlo-v1-alpha>

Second, we test the “Prior-like” model by using the denoising Transformer, but taking text guidance as input tokens instead of cross-attention. We also test two more CompoDiff models from our two-stage training strategy.

To measure the ability to understand raw text, we evaluate the models on image-to-text and text-to-image retrieval benchmarks on the MS-COCO Caption dataset [9]. We also evaluate them on the extension of COCO Caption to mitigate the false negative problem of COCO, namely, CxC [41] and ECCV Caption [14]. Table D.4 shows the average metrics of each benchmark for image-to-text and text-to-image. In the table, we first observe that our design choice is three times faster than the “Prior-ish” counterparts by handling textual embeddings with cross-attention. Second, we observe that Stage 1 only CompoDiff shows a better understanding of image-to-caption and caption-to-image retrieval tasks. We speculate that this is because Ours (Stage 1 only) is directly optimized by the image-to-text (ITM) matching style dataset, while Ours (Stage 1 + Stage 2) is also trained with other types of conditions (*e.g.*, masks, negative texts, image conditions).

The number of denoising steps. Since our CompoDiff is a diffusion model, denoising steps are required to denoise noisy image embeddings. However, it is possible to obtain reliable denoised image embeddings with just a few steps. As shown in Table D.5, we conducted a CIR evaluation on FashionIQ and it shows that even with only 5 iterations, our model can produce competitive results. If we use 100 steps, we have a slightly better performance (45.83 vs. 45.03 in the supervised scenario), but a much slower inference time (2.02 sec vs. 0.12 sec). Therefore, we can control the number of steps to improve the quality of the retrieved images and the inference time.

Condition strength As w_I increases, the generated image embeddings become more dependent on the reference



Figure D.1. More qualitative comparison of zero-shot CIR for Pic2Word and CompoDiff.

Method	COCO 5k			CxP			ECCV Caption			Throughput images/sec
	R@1	R@5	R@10	R@1	R@5	R@10	MAP@R	RPrecision	R@1	
Image to text retrieval										
Prior [31]	32.04	56.84	67.68	33.76	60.50	71.32	14.19	23.37	46.47	497.28
Prior-like Stage1	34.32	58.40	69.52	35.01	62.35	74.21	16.35	25.20	49.01	497.28
Ours (Stage 1 only)	35.13	59.46	70.26	35.30	62.62	74.02	16.01	25.44	49.64	1475.52
Ours (Stage 1 + Stage2)	33.20	58.00	68.94	34.78	61.68	72.96	15.07	24.39	47.03	1473.92
Text to image retrieval										
Prior [31]	17.05	34.25	43.16	18.62	37.43	47.07	18.10	26.46	46.40	497.28
Prior-like Stage1	22.62	38.31	48.11	21.42	41.42	51.79	20.70	29.80	51.50	497.28
Ours (Stage 1 only)	22.47	39.18	49.08	22.51	42.40	52.77	21.46	30.30	53.75	1475.52
Ours (Stage 1 + Stage2)	20.00	38.63	48.25	21.57	41.71	51.99	20.82	29.84	51.65	1473.92

Table D.4. Comparisons of various design choices for handling textual embeddings on text-to-image and image-to-text retrieval results on COCO, CxP and ECCV Caption datasets. For all metrics, higher is better.

image, while increasing w_T results in a greater influence of the text guidance. However, high-valued w_I and w_T are not always beneficial. If w_I or w_T is too high, it can lead to unwanted results. To find a harmonious combination of w_I and w_T , we performed a sweeping process as shown in Fig. D.2. We use w_I as 1.5 and w_T as 7.5 considering the best content-condition trade-off.

Data scale vs. performances. In this section, we performed stage 2 training while changing the size of the dataset by randomly sampling the 18.8M generated dataset. The results are shown in Table D.6. First, at a scale of 1M, the performance of CompoDiff trained on our 1M subset significantly outperformed that publicly provided by the authors of InstructPix2Pix [6]. This result indicates that our

Step	1	5	10	25	50	75	100
Zero-shot	21.52	42.17	42.33	41.42	42.45	42.61	42.65
Supervised	28.24	45.03	46.31	46.80	45.71	45.01	45.83
Time (sec)	0.02	0.12	0.23	0.56	1.08	1.62	2.02

Table D.5. **Performances vs. inference time by varying the number of denoising steps.** Numbers are measured on the FashionIQ validation split. “Ours” in Table 3 is equivalent to 10 steps.

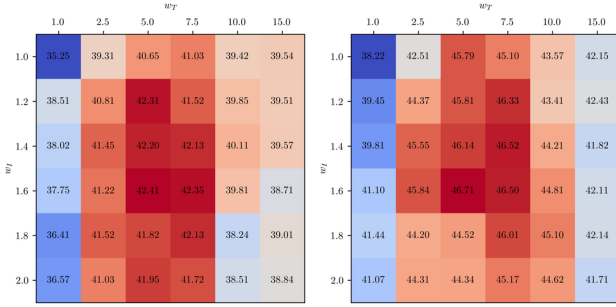


Figure D.2. **Fashion IQ CIR results by controlling w_T and w_I .** Red denotes higher scores and blue denotes lower scores.

	IP2P(1M) [6]	1M	5M	10M	18.8M
Zero-shot					
IN-R R@10	5.01	6.57	8.82	11.10	13.18
COCO R@1	7.87	8.29	8.69	8.73	8.71
FashionIQ	27.24	31.91	38.11	42.41	42.33
CIRR	11.41	11.20	16.87	22.30	22.88
Supervised					
FashionIQ	35.38	37.23	42.51	43.81	46.31
CIRR	23.62	24.01	26.88	27.21	27.52

Table D.6. **Dataset scale vs. performances.** We show all experimental results, including CIR tasks on FashionIQ and CIRR, domain conversion (Appendix D.2), and object conversion (Appendix D.3) tasks. IP2P denotes the public 1M synthetic dataset by Brooks *et al.* [6]. Otherwise, each model is trained by the subset of SynthTriplets18M.

dataset has a more diverse representation capability. As the size of our dataset increases, the performance gradually improves, and the overall performance is the best when using the entire dataset (18.8M).

Stage2 ablation. The reason for training with T2I retrieval and masked CIR together in stage 2 is not only to provide these features to users but also to serve as multi-task learners that enhance the representational ability of standard CIR. Although we generate triplets for CIR up to 18.8M scale it is clear that our generated dataset still lacks textual and visual representational ability compared to the LAION

dataset, which has a scale of billions. In order to include the LAION dataset in stage 2 training, we use the LAION dataset for T2I retrieval and masked CIR. Experimental results between stage 2 using only 18.8M generated dataset and the LAION dataset together are shown in Table D.7.

D.6. Image decoding using unCLIP generator.

unCLIP [47] consists of a prior module that converts text embeddings into image embeddings, a decoder that converts image embeddings into low-resolution images, and super-resolution models that convert low-resolution images into high-resolution images. As the official unCLIP model is not publicly available, we employ the community version of unCLIP. Fortunately, since the community unCLIP model uses embeddings from CLIP-L/14, we can directly use this model to generate images from the image embeddings generated by our CompoDiff. To do this, we simply replace Prior with CompoDiff. The generated images are shown in Fig. D.3, D.4, D.5, and D.6. To clarify, the unCLIP model is trained for **text-to-image** generation, not to edit input images and our CompoDiff generates image embeddings rather than generating images. As shown, the results are very promising. It seems that incorporating unCLIP into the search service could potentially improve the user experience by generating images when the desired search results are not available.

	<i>only Standard CIR</i>	T2I retrieval + Masked CIR + Standard CIR (proposed)
Zero-shot		
ImageNet-R R@10	12.58	13.18
COCO R@1	8.34	8.71
FashionIQ	41.15	42.33
CIRR	22.71	22.88
Supervised		
FashionIQ	45.14	46.31
CIRR	27.23	27.52

Table D.7. **Stage 2 ablation.** We compare the CIR-only training and our proposed multi-task learning in various tasks.

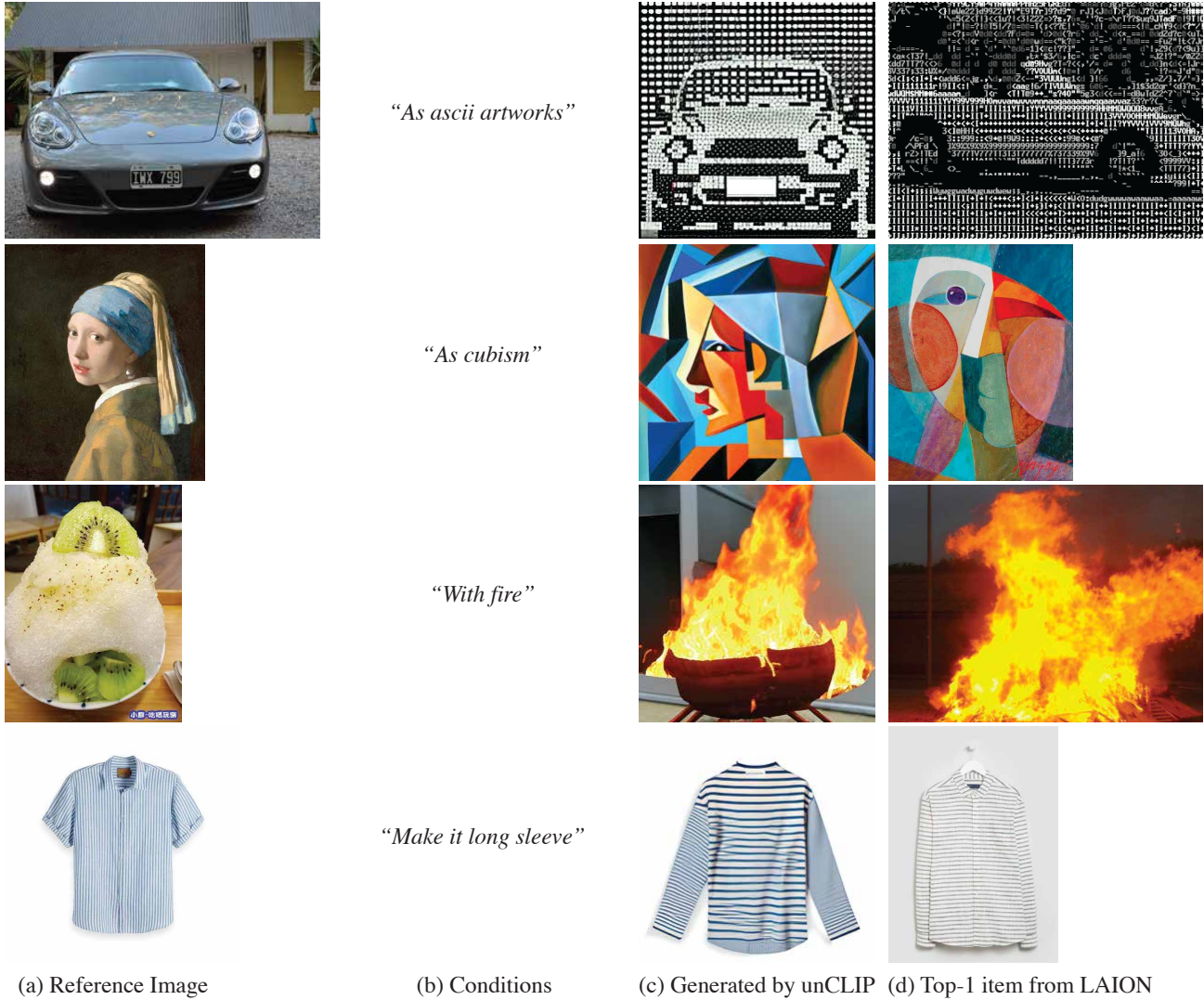
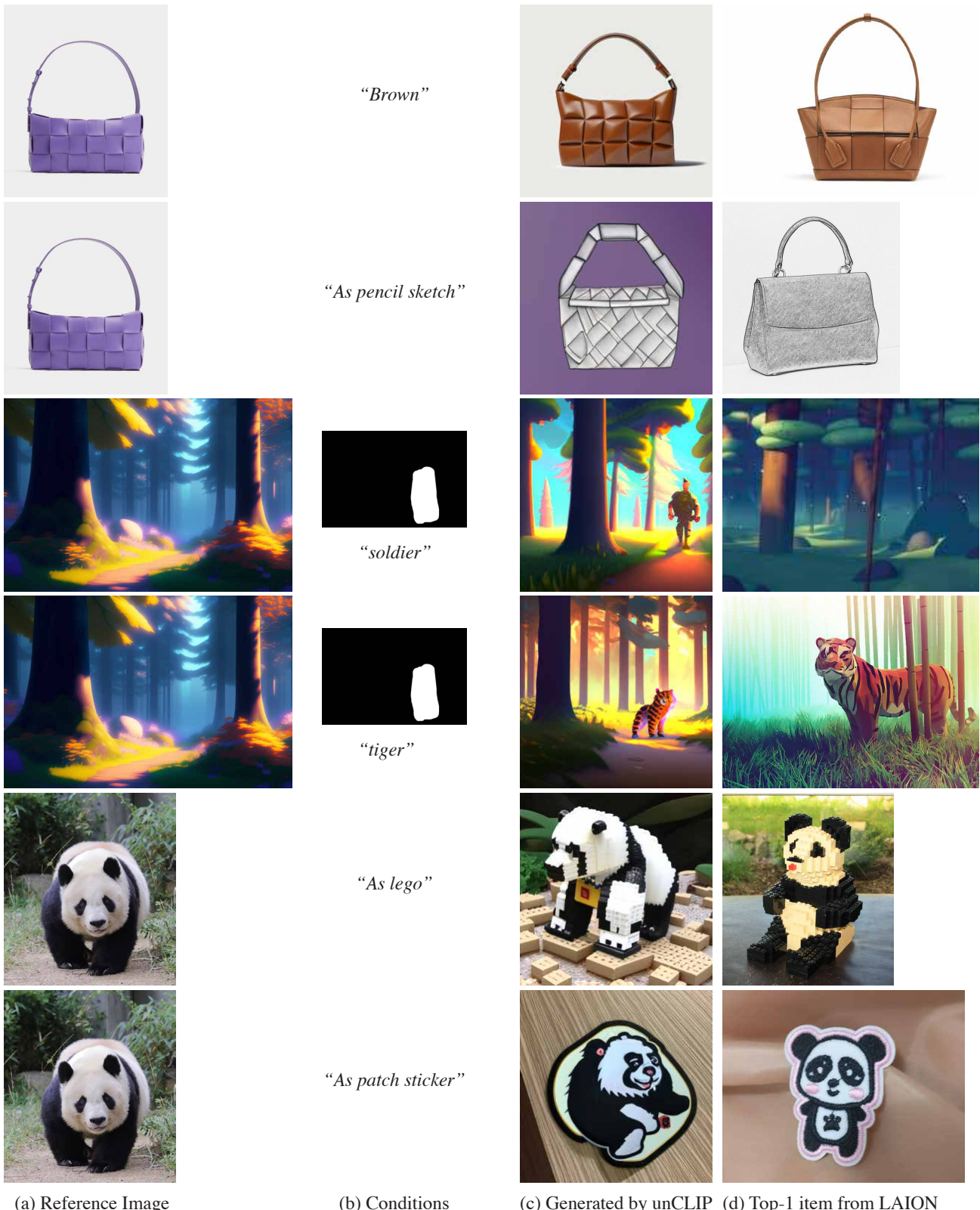


Figure D.3. **Generated vs. retrieved images by CompoDiff.** Using the transformed image feature by CompoDiff, we show a generated image using unCLIP [47] and top-1 retrieved image from LAION.



(a) Reference Image

(b) Conditions

(c) Generated by unCLIP (d) Top-1 item from LAION

Figure D.4. **Generated vs. retrieved images by CompoDiff (Continue).**



"Change her to spongebob"



"Change her to spongebob"
- *"surprised"*



"meteor"



"meteor"
- *"zoom out"*



"As 4k image"



"As 4k image"
- *"pink rabbit"*



(a) Reference Image

(b) Conditions

(c) Generated by unCLIP (d) Top-1 item from LAION

Figure D.5. **Generated vs. retrieved images by CompoDiff (Continue).**



"Made of ice"



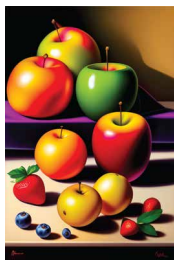
"Made of ice"
- *"Skill of artist"*



*"Drawn by a famous
artist from artstation"*



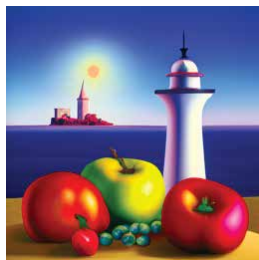
*"Drawn by a famous
artist from artstation"*
- *"Black and white"*



*"Add a lighthouse
in the background"*



"make the dog a cat"



(a) Reference Image

(b) Conditions

(c) Generated by unCLIP (d) Top-1 item from LAION

Figure D.6. Generated vs. retrieved images by CompoDiff (Continue).

References

- [1] Muhammad Umer Anwaar, Egor Labintcev, and Martin Kleinsteuber. Compositional learning of image-text query for image retrieval. (*arXiv:2006.11149*), May 2021. *arXiv:2006.11149 [cs]*. 2
- [2] Yogesh Balaji, Seungjun Nah, Xun Huang, Arash Vahdat, Jiaming Song, Karsten Kreis, Miika Aittala, Timo Aila, Samuli Laine, Bryan Catanzaro, et al. ediffi: Text-to-image diffusion models with an ensemble of expert denoisers. *arXiv preprint arXiv:2211.01324*, 2022. 12
- [3] Alberto Baldrati, Marco Bertini, Tiberio Uricchio, and Alberto Del Bimbo. Conditioned image retrieval for fashion using contrastive learning and clip-based features. In *ACM Multimedia Asia*, pages 1–5. 2021. 2
- [4] Alberto Baldrati, Marco Bertini, Tiberio Uricchio, and Alberto Del Bimbo. Conditioned and composed image retrieval combining and partially fine-tuning clip-based features. In *Proceedings of the IEEE/CVF Conference on Computer Vision and Pattern Recognition*, pages 4959–4968, 2022. 2, 6, 7, 8, 12, 14
- [5] Tamara L Berg, Alexander C Berg, and Jonathan Shih. Automatic attribute discovery and characterization from noisy web data. In *Computer Vision–ECCV 2010: 11th European Conference on Computer Vision, Heraklion, Crete, Greece, September 5–11, 2010, Proceedings, Part I 11*, pages 663–676. Springer, 2010. 3
- [6] Tim Brooks, Aleksander Holynski, and Alexei A Efros. Instructpix2pix: Learning to follow image editing instructions. *arXiv preprint arXiv:2211.09800*, 2022. 2, 3, 4, 15, 16
- [7] Minwoo Byeon, Beomhee Park, Haecheon Kim, Sungjun Lee, Woonhyuk Baek, and Saehoon Kim. Coyo-700m: Image-text pair dataset. <https://github.com/kakaobrain/coyo-dataset>, 2022. 3
- [8] Jiacheng Chen, Hexiang Hu, Hao Wu, Yuning Jiang, and Changhu Wang. Learning the best pooling strategy for visual semantic embedding. In *Proceedings of the IEEE/CVF conference on computer vision and pattern recognition*, pages 15789–15798, 2021. 2
- [9] Xinlei Chen, Hao Fang, Tsung-Yi Lin, Ramakrishna Vedantam, Saurabh Gupta, Piotr Dollár, and C Lawrence Zitnick. Microsoft coco captions: Data collection and evaluation server. *arXiv preprint arXiv:1504.00325*, 2015. 2, 3, 14
- [10] Yanbei Chen and Loris Bazzani. Learning joint visual semantic matching embeddings for language-guided retrieval. In *Computer Vision–ECCV 2020: 16th European Conference, Glasgow, UK, August 23–28, 2020, Proceedings, Part XXII 16*, pages 136–152. Springer, 2020. 7
- [11] Yanbei Chen, Shaogang Gong, and Loris Bazzani. Image search with text feedback by visiolinguistic attention learning. In *Proceedings of the IEEE/CVF Conference on Computer Vision and Pattern Recognition*, pages 3001–3011, 2020. 7
- [12] Yiyang Chen, Zhedong Zheng, Wei Ji, Leigang Qu, and Tat-Seng Chua. Composed image retrieval with text feedback via multi-grained uncertainty regularization. *arXiv preprint arXiv:2211.07394*, 2022. 2, 7
- [13] Junsuk Choe, Song Park, Kyungmin Kim, Joo Hyun Park, Dongseob Kim, and Hyunjung Shim. Face generation for low-shot learning using generative adversarial networks. In *Proceedings of the IEEE international conference on computer vision workshops*, pages 1940–1948, 2017. 3
- [14] Sanghyuk Chun, Wonjae Kim, Song Park, Minsuk Chang Chang, and Seong Joon Oh. Eccv caption: Correcting false negatives by collecting machine-and-human-verified image-caption associations for ms-coco. In *European Conference on Computer Vision (ECCV)*, 2022. 14
- [15] Sanghyuk Chun, Seong Joon Oh, Rafael Sampaio De Rezende, Yannis Kalantidis, and Diane Larlus. Probabilistic embeddings for cross-modal retrieval. In *Conference on Computer Vision and Pattern Recognition (CVPR)*, 2021. 2
- [16] Ginger Delmas, Rafael S Rezende, Gabriela Csurka, and Diane Larlus. Artemis: Attention-based retrieval with text-explicit matching and implicit similarity. In *International Conference on Learning Representations*, 2022. 2, 6, 7, 8, 12, 14
- [17] Eric Dodds, Jack Culpepper, Simao Herdade, Yang Zhang, and Kofi Boakye. Modality-agnostic attention fusion for visual search with text feedback. *arXiv preprint arXiv:2007.00145*, 2020. 7, 8
- [18] Fartash Faghri, David J Fleet, Jamie Ryan Kiros, and Sanja Fidler. Vse++: Improving visual-semantic embeddings with hard negatives. In *Proceedings of the British Machine Vision Conference (BMVC)*, 2018. 1, 2
- [19] Xiaoxiao Guo, Hui Wu, Yu Cheng, Steven Rennie, Gerald Tesuero, and Rogerio Feris. Dialog-based interactive image retrieval. In *Advances in neural information processing systems*, volume 31, 2018. 3
- [20] Xintong Han, Zuxuan Wu, Phoenix X Huang, Xiao Zhang, Menglong Zhu, Yuan Li, Yang Zhao, and Larry S Davis. Automatic spatially-aware fashion concept discovery. In *Proceedings of the IEEE international conference on computer vision*, pages 1463–1471, 2017. 3
- [21] Dan Hendrycks, Steven Basart, Norman Mu, Saurav Kadavath, Frank Wang, Evan Dorundo, Rahul Desai, Tyler Zhu, Samyak Parajuli, Mike Guo, et al. The many faces of robustness: A critical analysis of out-of-distribution generalization. In *Proceedings of the IEEE/CVF International Conference on Computer Vision*, pages 8340–8349, 2021. 7, 12
- [22] Amir Hertz, Ron Mokady, Jay Tenenbaum, Kfir Aberman, Yael Pritch, and Daniel Cohen-Or. Prompt-to-prompt image editing with cross attention control. *arXiv preprint arXiv:2208.01626*, 2022. 3, 4
- [23] Jonathan Ho, Ajay Jain, and Pieter Abbeel. Denoising diffusion probabilistic models. *Advances in Neural Information Processing Systems*, 33:6840–6851, 2020. 3, 5
- [24] Jonathan Ho and Tim Salimans. Classifier-free diffusion guidance. *arXiv preprint arXiv:2207.12598*, 2022. 3, 5
- [25] Surgan Jandial, Pinkesh Badjatiya, Pranit Chawla, Ayush Chopra, Mausoom Sarkar, and Balaji Krishnamurthy. Sac: Semantic attention composition for text-conditioned image retrieval. In *Proceedings of the IEEE/CVF Winter Conference on Applications of Computer Vision*, pages 4021–4030, 2022. 7

- [26] Surgan Jandial, Ayush Chopra, Pinkesh Badjatiya, Pranit Chawla, Mausoom Sarkar, and Balaji Krishnamurthy. Trace: Transform aggregate and compose visiolinguistic representations for image search with text feedback. *arXiv preprint arXiv:2009.01485*, 7, 2020. 7
- [27] Chao Jia, Yinfei Yang, Ye Xia, Yi-Ting Chen, Zarana Parekh, Hieu Pham, Quoc V. Le, Yunhsuan Sung, Zhen Li, and Tom Duerig. *Scaling Up Visual and Vision-Language Representation Learning With Noisy Text Supervision*. Number arXiv:2102.05918. Jun 2021. arXiv:2102.05918 [cs] type: article. 2
- [28] Jeff Johnson, Matthijs Douze, and Hervé Jégou. Billion-scale similarity search with gpus. *IEEE Transactions on Big Data*, 7(3):535–547, 2019. 6, 7
- [29] Jongseok Kim, Youngjae Yu, Hoeseong Kim, and Gunhee Kim. Dual compositional learning in interactive image retrieval. In *Proceedings of the AAAI Conference on Artificial Intelligence*, volume 35, pages 1771–1779, 2021. 7
- [30] Alina Kuznetsova, Hassan Rom, Neil Alldrin, Jasper Uijlings, Ivan Krasin, Jordi Pont-Tuset, Shahab Kamali, Stefan Popov, Matteo Malloci, Alexander Kolesnikov, et al. The open images dataset v4: Unified image classification, object detection, and visual relationship detection at scale. *International Journal of Computer Vision*, 128(7):1956–1981, 2020. 13
- [31] Donghoon Lee, Jiseob Kim, Jisu Choi, Jongmin Kim, Minwoo Byeon, Woonhyuk Baek, and Saehoon Kim. Karlov1.0.alpha on coyo-100m and cc15m. <https://github.com/kakaobrain/karlo>, 2022. 15
- [32] Kimin Lee, Honglak Lee, Kibok Lee, and Jinwoo Shin. Training confidence-calibrated classifiers for detecting out-of-distribution samples. In *International Conference on Learning Representations*, 2018. 3
- [33] Seungmin Lee, Dongwan Kim, and Bohyung Han. Cosmo: Content-style modulation for image retrieval with text feedback. In *Proceedings of the IEEE/CVF Conference on Computer Vision and Pattern Recognition*, pages 802–812, 2021. 7
- [34] Junnan Li, Dongxu Li, Caiming Xiong, and Steven Hoi. Blip: Bootstrapping language-image pre-training for unified vision-language understanding and generation. In *International Conference on Machine Learning*, pages 12888–12900. PMLR, 2022. 2
- [35] Tsung-Yi Lin, Michael Maire, Serge Belongie, James Hays, Pietro Perona, Deva Ramanan, Piotr Dollár, and C Lawrence Zitnick. Microsoft coco: Common objects in context. In *Computer Vision–ECCV 2014: 13th European Conference, Zurich, Switzerland, September 6–12, 2014, Proceedings, Part V 13*, pages 740–755. Springer, 2014. 7, 13
- [36] Zheyuan Liu, Cristian Rodriguez-Opazo, Damien Teney, and Stephen Gould. Image retrieval on real-life images with pre-trained vision-and-language models. In *Proceedings of the IEEE/CVF International Conference on Computer Vision*, pages 2125–2134, 2021. 1, 3, 6, 9, 13
- [37] Zheyuan Liu, Cristian Rodriguez-Opazo, Damien Teney, and Stephen Gould. Image retrieval on real-life images with pre-trained vision-and-language models. In *Proceedings of the IEEE/CVF International Conference on Computer Vision*, pages 2125–2134, 2021. 7, 8
- [38] Ilya Loshchilov and Frank Hutter. Decoupled weight decay regularization. *arXiv preprint arXiv:1711.05101*, 2017. 12, 13
- [39] Timo Lüddecke and Alexander Ecker. Image segmentation using text and image prompts. In *Proceedings of the IEEE/CVF Conference on Computer Vision and Pattern Recognition*, pages 7086–7096, 2022. 5
- [40] Nithin Gopalakrishnan Nair, Wele Gedara Chaminda Bandara, and Vishal M. Patel. Unite and conquer: Cross dataset multimodal synthesis using diffusion models. (arXiv:2212.00793), Dec 2022. arXiv:2212.00793 [cs]. 3
- [41] Zarana Parekh, Jason Baldridge, Daniel Cer, Austin Walters, and Yinfei Yang. Crisscrossed captions: Extended intramodal and intermodal semantic similarity judgments for ms-coco. *arXiv preprint arXiv:2004.15020*, 2020. 14
- [42] William Peebles and Saining Xie. Scalable diffusion models with transformers. *arXiv preprint arXiv:2212.09748*, 2022. 12
- [43] James Philbin, Ondrej Chum, Michael Isard, Josef Sivic, and Andrew Zisserman. Object retrieval with large vocabularies and fast spatial matching. In *2007 IEEE conference on computer vision and pattern recognition*, pages 1–8. IEEE, 2007. 1
- [44] Alec Radford, Jong Wook Kim, Chris Hallacy, Aditya Ramesh, Gabriel Goh, Sandhini Agarwal, Girish Sastry, Amanda Askell, Pamela Mishkin, Jack Clark, et al. Learning transferable visual models from natural language supervision. In *International conference on machine learning*, pages 8748–8763. PMLR, 2021. 1, 2, 13
- [45] Colin Raffel, Noam Shazeer, Adam Roberts, Katherine Lee, Sharan Narang, Michael Matena, Yanqi Zhou, Wei Li, and Peter J Liu. Exploring the limits of transfer learning with a unified text-to-text transformer. *The Journal of Machine Learning Research*, 21(1):5485–5551, 2020. 6, 7, 8
- [46] Colin Raffel, Noam Shazeer, Adam Roberts, Katherine Lee, Sharan Narang, Michael Matena, Yanqi Zhou, Wei Li, and Peter J Liu. Exploring the limits of transfer learning with a unified text-to-text transformer. *The Journal of Machine Learning Research*, 21(1):5485–5551, 2020. 12
- [47] Aditya Ramesh, Prafulla Dhariwal, Alex Nichol, Casey Chu, and Mark Chen. Hierarchical text-conditional image generation with clip latents. *arXiv preprint arXiv:2204.06125*, 2022. 2, 5, 6, 8, 9, 14, 16, 17
- [48] Robin Rombach, Andreas Blattmann, Dominik Lorenz, Patrick Esser, and Björn Ommer. High-resolution image synthesis with latent diffusion models. In *Proceedings of the IEEE/CVF Conference on Computer Vision and Pattern Recognition*, pages 10684–10695, 2022. 2, 3, 4, 12
- [49] Olga Russakovsky, Jia Deng, Hao Su, Jonathan Krause, Sanjeev Satheesh, Sean Ma, Zhiheng Huang, Andrej Karpathy, Aditya Khosla, Michael Bernstein, et al. Imagenet large scale visual recognition challenge. *International journal of computer vision*, 115:211–252, 2015. 12
- [50] Kuniaki Saito, Kihyuk Sohn, Xiang Zhang, Chun-Liang Li, Chen-Yu Lee, Kate Saenko, and Tomas Pfister. Pic2word:

- Mapping pictures to words for zero-shot composed image retrieval. *arXiv preprint arXiv:2302.03084*, 2023. 1, 2, 6, 7, 8, 12, 13, 14
- [51] Veit Sandfort, Ke Yan, Perry J Pickhardt, and Ronald M Summers. Data augmentation using generative adversarial networks (cyclegan) to improve generalizability in ct segmentation tasks. *Scientific reports*, 9(1):16884, 2019. 3
- [52] Christoph Schuhmann, Romain Beaumont, Richard Vencu, Cade Gordon, Ross Wightman, Mehdi Cherti, Theo Coombes, Aarush Katta, Clayton Mullis, Mitchell Wortsman, et al. Laion-5b: An open large-scale dataset for training next generation image-text models. *arXiv preprint arXiv:2210.08402*, 2022. 3, 5, 6, 7, 12, 13, 14
- [53] Christoph Schuhmann, Andreas Köpf, Richard Vencu, Theo Coombes, and Romain Beaumont. Laion coco: 600m synthetic captions from laion2b-en. <https://huggingface.co/datasets/laion/laion-coco>, 2022. 3
- [54] Piyush Sharma, Nan Ding, Sebastian Goodman, and Radu Soricut. Conceptual captions: A cleaned, hypernymed, image alt-text dataset for automatic image captioning. In *Proceedings of the 56th Annual Meeting of the Association for Computational Linguistics (Volume 1: Long Papers)*, pages 2556–2565, 2018. 13, 14
- [55] Minchul Shin, Yoonjae Cho, Byungsoo Ko, and Geonmo Gu. Rtic: Residual learning for text and image composition using graph convolutional network. *arXiv preprint arXiv:2104.03015*, 2021. 7
- [56] Jordan Shipard, Arnold Wiliem, Kien Nguyen Thanh, Wei Xiang, and Clinton Fookes. Boosting zero-shot classification with synthetic data diversity via stable diffusion. (*arXiv:2302.03298*), Feb 2023. *arXiv:2302.03298 [cs]*. 3
- [57] Jiaming Song, Chenlin Meng, and Stefano Ermon. Denoising diffusion implicit models. *arXiv preprint arXiv:2010.02502*, 2020. 13
- [58] Yale Song and Mohammad Soleymani. Polysemous visual-semantic embedding for cross-modal retrieval. In *Proceedings of the IEEE/CVF Conference on Computer Vision and Pattern Recognition*, pages 1979–1988, 2019. 2
- [59] Alane Suhr, Stephanie Zhou, Ally Zhang, Iris Zhang, Hua-jun Bai, and Yoav Artzi. A corpus for reasoning about natural language grounded in photographs. *arXiv preprint arXiv:1811.00491*, 2018. 3
- [60] Yuxin Tian, Shawn Newsam, and Kofi Boakye. Image search with text feedback by additive attention compositional learning. *arXiv preprint arXiv:2203.03809*, 2022. 7
- [61] Ashish Vaswani, Noam Shazeer, Niki Parmar, Jakob Uszkoreit, Llion Jones, Aidan N Gomez, Łukasz Kaiser, and Illia Polosukhin. Attention is all you need. *Advances in neural information processing systems*, 30, 2017. 12
- [62] Nam Vo, Lu Jiang, Chen Sun, Kevin Murphy, Li-Jia Li, Li Fei-Fei, and James Hays. Composing text and image for image retrieval—an empirical odyssey. In *Proceedings of the IEEE/CVF conference on computer vision and pattern recognition*, pages 6439–6448, 2019. 2, 6, 8
- [63] Hui Wu, Yupeng Gao, Xiaoxiao Guo, Ziad Al-Halah, Steven Rennie, Kristen Grauman, and Rogerio Feris. Fashion iq: A new dataset towards retrieving images by natural language feedback. In *Proceedings of the IEEE/CVF Conference on Computer Vision and Pattern Recognition*, pages 11307–11317, 2021. 1, 3, 6, 9, 13
- [64] Youngjae Yu, Seunghwan Lee, Yuncheol Choi, and Gun-hee Kim. Curlingnet: Compositional learning between images and text for fashion iq data. *arXiv preprint arXiv:2003.12299*, 2020. 2, 7
- [65] Susan Zhang, Stephen Roller, Naman Goyal, Mikel Artetxe, Moya Chen, Shuhui Chen, Christopher Dewan, Mona Diab, Xian Li, Xi Victoria Lin, et al. Opt: Open pre-trained transformer language models. *arXiv preprint arXiv:2205.01068*, 2022. 2, 3, 4